

A Novel Pathway of Cytochrome *c* Biogenesis Is Involved in the Assembly of the Cytochrome *b₆f* Complex in *Arabidopsis* Chloroplasts^{*[5]}

Received for publication, May 20, 2008, and in revised form, June 30, 2008 Published, JBC Papers in Press, July 1, 2008, DOI 10.1074/jbc.M803869200

Lina Lezhneva^{‡§1}, Richard Kuras^{‡§}, Geneviève Ephritikhine^{¶||}, and Catherine de Vitry^{‡§2}

From the [‡]CNRS, UMR 7141, Laboratoire de Physiologie Membranaire et Moléculaire du Chloroplaste, Institut de Biologie Physico-Chimique, 13 Rue Pierre et Marie Curie, 75005 Paris, France, the [§]UPMC Université de Paris 06, UMR 7141, F-75005, Paris, France, the [¶]CNRS, UPR 2355, Institut des Sciences du Végétal, 1 Avenue de la Terrasse, 91198 Gif-sur-Yvette Cedex, France, and the ^{||}Université Paris-Diderot, UFR Sciences du Vivant, 2 Place Jussieu, 75251 Paris Cedex 05, France

We recently characterized a novel heme biogenesis pathway required for heme *c*_i' covalent binding to cytochrome *b₆* in *Chlamydomonas* named system IV or CCB (cofactor assembly, complex C (*b₆f*), subunit B (PetB)). To find out whether this CCB pathway also operates in higher plants and extend the knowledge of the *c*-type cytochrome biogenesis, we studied *Arabidopsis* insertion mutants in the orthologs of the CCB genes. The *ccb1*, *ccb2*, and *ccb4* mutants show a phenotype characterized by a deficiency in the accumulation of the subunits of the cytochrome *b₆f* complex and lack covalent heme binding to cytochrome *b₆*. These mutants were functionally complemented with the corresponding wild type cDNAs. Using fluorescent protein reporters, we demonstrated that the CCB1, CCB2, CCB3, and CCB4 proteins are targeted to the chloroplast compartment of *Arabidopsis*. We have extended our study to the YGGT family, to which CCB3 belongs, by studying insertion mutants of two additional members of this family for which no mutants were previously characterized, and we showed that they are not functionally involved in the CCB system. Thus, we demonstrate the ubiquity of the CCB proteins in chloroplast heme *c*_i' binding.

The cytochrome *b₆f* complex is a large multisubunit pigment-protein complex located in the photosynthetic membranes of cyanobacteria, algae, and vascular plants. It has a plastoquinol-plastocyanin/cytochrome *c₆* oxidoreductase activity and mediates the electron transfer between photosystems II and I. The electron flow through the cytochrome *b₆f* complex is coupled to the translocation of protons, thereby contributing to ATP synthesis (reviewed in Refs. 1 and 2). The cytochrome *b₆f* complex also regulates the use of light energy by playing a role in the processes of state transition and redox regulation (3–7), cyclic electron flow, and photoprotection (8, 9).

The crystal structure of the cytochrome *b₆f* complex in a cyanobacterium and a green alga revealed its highly conserved organization (10, 11). It forms a functional dimer comprising four large and four smaller subunits and binding several cofactors. Two heme prosthetic groups are covalently bound to the protein moieties: the heme *c* of cytochrome *f* and the newly discovered heme *c*_i' attached to cytochrome *b₆* in the quinone-binding site Q_i (referred as *c*_i in Refs. 10 and 11). This additional heme was first identified by *in vivo* spectroscopy as a redox center in equilibrium with heme *b_h*, named "G" and proposed to be located near the stromal side of the membrane (12). G was later characterized as a cytochrome *c*' (13) and is hereafter referred to as heme *c*_i'. Typical members of the *c*-type cytochrome family, to which cytochrome *f* belongs, are characterized by (i) covalent ligation via two thioether bonds of the heme vinyl groups to two cysteinyl residues located in a highly conserved CXXCH motif of the protein and (ii) a hexacoordinated heme iron with two amino acid residues of the protein providing the heme axial ligands, one of them being the histidyl residue of the CXXCH motif.

Interestingly, the covalently bound heme of cytochrome *b₆* differs from the majority of the *c*-type cytochrome family hemes (10, 11, 14). In cytochrome *b₆*, this heme is pentacoordinated and therefore high spin, hence the designation of *c*_i', and covalently attached by a single thioether bond to the protein backbone (15–19). The unique heme iron axial ligand is not provided by the side chain of amino acid residue but by a water or hydroxyl molecule that bridges the heme iron of heme *c*_i' to the carboxyl group of one of the propionates of heme *b_h*.

Hemes are hydrophobic and cytotoxic macrocycles that require specific pathways for their delivery to subcellular destinations. Three distinct pathways, comprising several protein components and referred to as systems I, II, and III described in bacteria, chloroplasts, and mitochondria are involved in the assembly of *c*-type cytochromes located on the positively charged side of the membrane, opposite to the side where membrane insertion of the protein backbone occurs (20–22). Indications that the maturation of cytochrome *b₆* was not spontaneous and differed from other known maturation systems came from previous biochemical studies showing that at least four protein factors, encoded by the nuclear genome, were necessary to covalently attach a heme to cytochrome *b₆*. The genes

^{*} This work was supported in part by the CNRS, the UPMC Université Paris 6, and the Université Paris-Diderot. The costs of publication of this article were defrayed in part by the payment of page charges. This article must therefore be hereby marked "advertisement" in accordance with 18 U.S.C. Section 1734 solely to indicate this fact.

^[5] The on-line version of this article (available at <http://www.jbc.org>) contains supplemental Tables S1 and S2.

¹ Supported by a post-doctoral fellowship from the CNRS.

² To whom correspondence should be addressed. Tel.: 33-1-58-41-50-55; Fax: 33-1-58-41-50-22; E-mail: catherine.devitry@ibpc.fr.

encoding these proteins were referred to as the CCB genes for cofactor assembly of complex C (cytochrome *b₆*f) targeting subunit B (cytochrome *b₆* encoded by the *petB* gene) (23). Recently, four CCB genes were characterized in *Chlamydomonas*, and their analysis revealed not only that they described a new maturation pathway for *c*-type cytochromes located on the negatively charged side (n-side) of the membrane but also that the CCB pathway should be conserved among organisms performing oxygenic photosynthesis (24). These four CCB proteins had no previously identified conserved domains except CCB3, which belongs to the YGGT protein family. The YGGT protein family (European Molecular Biology Laboratory InterPro accession number IPR003425) was named after the *Escherichia coli* *yggT* gene. The YGGT repeat is found in conserved hypothetical integral membrane proteins present in bacteria and chloroplasts and has an unknown function. Photosynthetic eukaryotes contain up to four YGGT members (three in *Chlamydomonas* and four in *Arabidopsis*), all predicted to be chloroplast-localized.

To extend knowledge on the biogenesis of *c*-type cytochromes and explore the role of the CCB proteins in higher plants, *Arabidopsis* mutants of three *Chlamydomonas* CCB gene orthologs were analyzed (no *Arabidopsis* mutants altered in the CCB3 gene were available). Using protein fluorescent reporters, we show that the four CCB proteins are targeted to *Arabidopsis* chloroplasts. We have also studied insertion mutants in other members of the YGGT protein family for which no *Chlamydomonas* mutants were available. Our results clearly indicate that the function of the CCB proteins is conserved in *Arabidopsis*, demonstrating that the CCB pathway can be regarded as generalized for holocytochrome *b₆* assembly in chloroplasts.

EXPERIMENTAL PROCEDURES

Plant Growth and Selection—The mutant *ccb* and *yggT-b* lines (see supplemental Table S1), ecotype Columbia, were from the collection of the Salk Institute, (La Jolla, CA). The *yggT-a* line, ecotype Columbia, was from the collection of the University of Wisconsin (Madison, WI). Seeds were obtained from the Nottingham *Arabidopsis* Stock Centre. Seed sterilization and growth conditions for wild type and mutant plants were described in Ref. 25. Plants were grown under continuous light at a photon flux density of 40–50 $\mu\text{E m}^{-2} \text{s}^{-1}$ for 20 days on sterile medium containing 1 \times murashige and skoog salts (26), 1.5% (w/v) sucrose, 2.5 mM MES- NaOH ,³ pH 5.7, and 0.3% (w/v) Gelrite. Mutants were selected according to fluorescence induction kinetics measured with an in-house built set-up described in Ref. 27. To have the same genetic background, phenotypically wild type plants of progenies of heterozygous lines grown under the same conditions were compared with mutants in all experiments. Propagation of the seedling-lethal *ccb* mutants occurred via heterozygous offspring grown on soil.

To prove the T-DNA insertion sites, PCR analyses were performed using primers specific for the T-DNA, LB, and the gene of interest, *ccb1-f*, *ccb2-r2*, and *ccb4-f1* for the *CCB1*, *CCB2*,

and *CCB4* genes, respectively (supplemental Table S2 and Fig. 1). To select homozygous mutants, gene-specific primer combinations *ccb1-f/ccb1-r*, *ccb2-f2/ccb2-r2*, and *ccb4-f1/ccb4-r1* were used for *CCB1*, *CCB2*, and *CCB4* genes, respectively (supplemental Table S2 and Fig. 1). The T-DNA insertion prevented PCR amplification of the corresponding locus in the homozygous lines. Actin-*f* and actin-*r* primers (supplemental Table S2), which amplify the *At2g37620* actin 1 gene locus, were used in combination with the gene-specific primers as an internal PCR control.

cDNA Clones—The cDNAs of *CCB1* (RAFL09-81-B07), *CCB2* (RAFL21-80-A07), *CCB3* (RAFL06-10-D06), and *CCB4* (RAFL21-69-K09 and RAFL25-07-B10) were obtained from the RIKEN BioResource Center (28, 29). The RAFL25-07-B10 *CCB4* cDNA arose as a result of alternative splicing and carried the unspliced intron 6 and rearrangements in the 3'-untranslated region.

Complementation of the *ccb* Mutants—The full-size *CCB1*, *CCB2*, and *CCB4* cDNAs were amplified using the Expand High Fidelity^{PLUS} PCR System (Roche Applied Science). For the amplification of the *CCB1* cDNA, the *ccb1-Bam-f* and *ccb1-Xba-r* oligonucleotide primers (supplemental Table S2) were used, introducing BamHI (for the former) and XbaI (for the latter) restriction sites. After digestion with BamHI and XbaI and purification, the PCR product was ligated into the BamHI/XbaI sites of the plant binary expression vector pSEX001-VS (30). The result of cloning was verified by sequencing. The construct for the *ccb2* complementation was done in the same way using the *ccb2-Bam-f* and *ccb2-Xba-r* primers (supplemental Table S2). The two *CCB4* cDNA were amplified using the *ccb4-Bam-f/ccb4-Bam-r1* and *ccb4-Bam-f/ccb4-Bam-r2* primer combinations. The resulting fragments were cloned into the BamHI site of the vector pSEX001-VS. The obtained constructs were introduced into *Agrobacterium tumefaciens* GV3101 (pMP90RK) (31) and transformed into progenies of heterozygous plants using the floral dip method (32). Selection of transformants was performed on rock wool (Grodan, Hobro, Denmark) soaked in one-quarter strength murashige and skoog medium (26) supplemented with 10 mg/liter sulfadiazine (33). Homozygosity and the T-DNA insertion in resistant complemented lines was confirmed as described above. The presence of the cDNA was analyzed by PCR using exon-specific primers *ccb1-f/ccb1-r1* for *CCB1*, *ccb2-f1/ccb2-r1* for *CCB2*, *ccb4-f2/ccb4-r2*, and *ccb4-f3/ccb4-r3* for *CCB4.1* and *CCB4.2*, respectively.

Subcellular Localization—cDNA sequences encoding full-length CCB1 and CCB3 proteins and putative transit peptides of the CCB2 and CCB4 proteins were amplified using the Expand High Fidelity^{PLUS} PCR System (Roche Applied Science) and *ccb1-Kpn-f/ccb1-Kpn-r*, *ccb2-Kpn-f/ccb2-Kpn-r*, *ccb3-Sal-f/ccb3-Sal-r*, and *ccb4-Sal-f/ccb4-Sal-r* primer combinations (supplemental Table S2) for the *CCB1*, *CCB2*, *CCB3*, and *CCB4* genes, respectively. The amplified *CCB1* and *CCB2* fragments were digested with KpnI, and the *CCB3* and *CCB4* fragments were cut with SalI. After purification, the *CCB1*, *CCB3*, and *CCB4* products were cloned in-frame into the KpnI or SalI site of the GFP expression vector pOL-LT (34). The *CCB2* was introduced in-frame into the RFP expression

³ The abbreviations used are: MES, 2-(*N*-morpholino)ethanesulfonic acid; WT, wild type; GFP, green fluorescent protein; RFP, red fluorescent protein.

CCB Pathway in *Arabidopsis*

vector pOL-DsRed (34). Transient expression was performed in polyethylene glycol-treated protoplasts of *Arabidopsis* cell suspension (35).

Fluorescence was visualized 16 h after transformation, using a confocal laser scanning microscope (Leica TCS SP2; Leica Microsystems, Wetzlar, Germany). GFP was excited at 488 nm, and the fluorescence emission signal was detected between 500 and 535 nm. The RFP fusion construct was excited at 543 nm, and the emission signal was recovered between 570 and 637 nm. Chlorophyll autofluorescence was recorded between 675 and 750 nm.

Protein Analyses—Membrane proteins of wild type and mutant plants were isolated as described in Ref. 25. Protein separation on 12–18% SDS-polyacrylamide gels, electrotransfer, immunoblotting, and heme staining on blots using chemiluminescence were performed as described in Refs. 15 and 24. After transfer, membrane-bound proteins were stained using Coomassie Brilliant Blue according to the manufacturer's instructions (WESTRAN® Clear Signal protein transfer blotting membrane; Whatman®; Schleicher & Schuell). Protein amounts of mutants were adjusted to protein amounts in wild type having 8.5 μ g of chlorophyll. Chlorophyll concentrations were measured according to Ref. 36. For Western blot analyses antisera raised against the whole higher plant cytochrome *b*₆, AtpC and PsbA proteins (at a dilution of 1:5000), PsbA (Agrisera, Vännäs, Sweden; catalog number AS05084 at a 1:20,000 dilution), and *Chlamydomonas* cytochrome *f* (antiserum raised against the entire polypeptide at a 1:10,000 dilution) were used.

RESULTS

The Conservation of the CCB Genes in *Arabidopsis*—The four CCB proteins, which were recently implicated in heme *c*_i' biogenesis in the unicellular green alga *Chlamydomonas* are conserved in all organisms performing oxygenic photosynthesis whose genomic sequences are available (24). The *Chlamydomonas* CCB2 and CCB4 proteins are paralogous proteins with an amino acid identity of 30% using BLAST 2 sequences algorithm (37). The *Arabidopsis* genome comprises orthologs for CCB1 (AT3G26710) and CCB3 (AT5G36120) as well as for the paralogous CCB2 (AT5G52110) and CCB4 (AT1G59840) genes (genes in Fig. 1 and proteins in Fig. 2A). The two alternative spliced gene models for CCB2 are translated in exactly the same protein. In contrast, the second gene model for CCB4 corresponds to a shorter cDNA and is translated as a protein lacking the last 57 amino acids (indicated in CCB4 protein sequence in *italic* in Fig. 2A). The encoded *Arabidopsis* proteins share high similarity with their *Chlamydomonas* counterparts. Amino acid identity of 37, 30, 52, and 42% for the CCB1, CCB2, CCB3, and CCB4 full-length proteins could be identified using a BLAST 2 sequences algorithm (37).

The CCB proteins are encoded in the nucleus genome of *Arabidopsis* and have chloroplast transit peptides indicated in Fig. 2A as predicted by the ChloroP (38). Experimental evidence sustaining the chloroplast membrane localization of the CCB proteins is their immunodetection in chloroplast membranes of *Chlamydomonas* (24), their targeting to *Arabidopsis* chloroplasts using fluorescence protein reporters

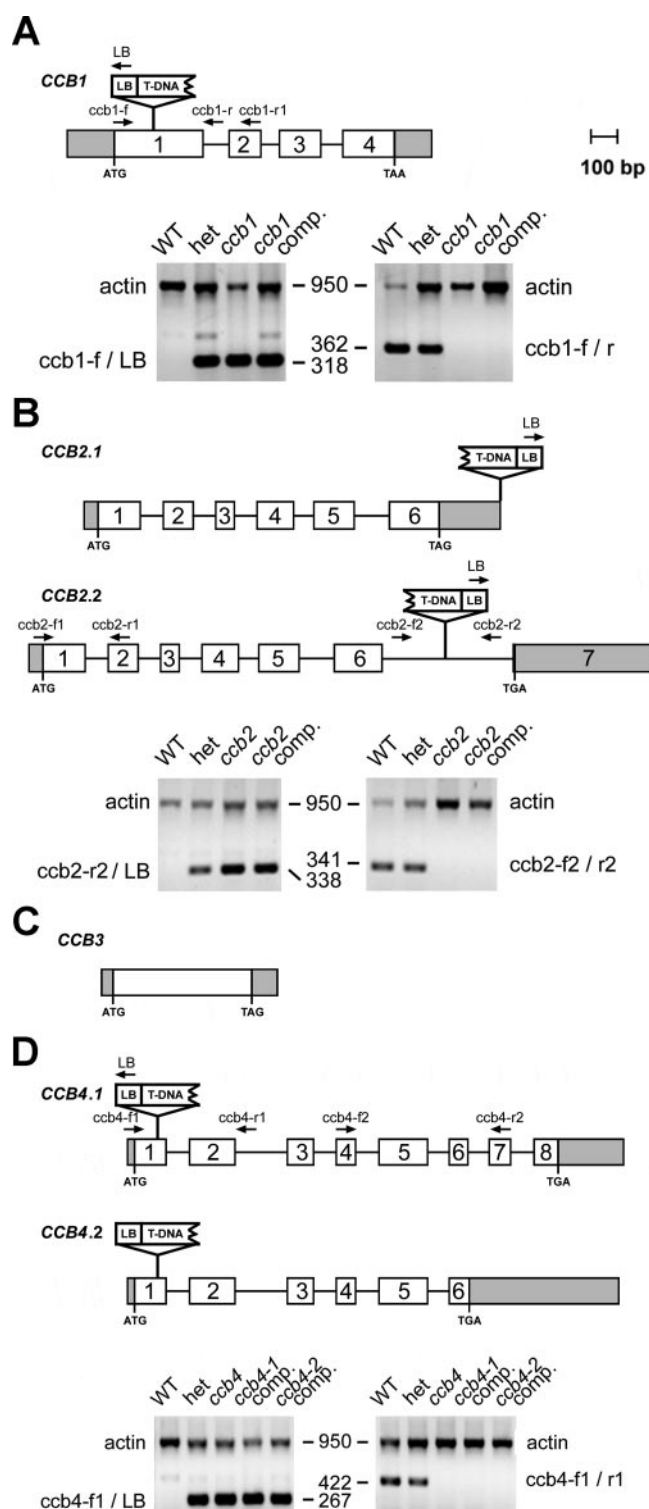


FIGURE 1. Schematic representations of the CCB1, CCB2, CCB3, and CCB4 genes in *Arabidopsis*. The sites of T-DNA insertion in mutants *ccb1* (A), *ccb2* (B), and *ccb4* (D) are shown above each gene model. The sites of the primers used for PCR analyses are indicated by *small arrows*. The lower part of each panel shows the results of PCR analyses of the T-DNA insertion. For each panel, analyses were performed on genomic DNA of WT, heterozygous (*het*), and homozygous mutant lines obtained by self-pollination of heterozygous *ccb1* (A), *ccb2* (B), and *ccb4* (D) mutants. PCR analyses of each *ccb* mutant complemented (*ccb comp*) with the corresponding wild type cDNAs are also shown. Amplification of actin was used as an internal control for the PCR experiments. Note that primers located in introns were used to avoid the amplification of the cDNA in the complemented lines and demonstrate the homozygosity of the mutations. No mutants altered in the CCB3 gene were available (C).

A

CCB1

MTAKLISPPFLSCPVVTSREVIKGLPRRRREWMVTKNRVSAVTAMIVEPLSVVSSSAIQ
IHQWQONPNSLLMTTEATGGYSLASYTSLGLFVIVPGLWSLIKRSVKSKIVKTFVV
NDVKKEPKQVAGEILSFFTRKNFNITDRGETITFEKGMVPSRGQAALLTFCTCISLASVG
LVLITIVPDPFGNNWFFIILLSPLAGVYWKASRKEIKVKMMVSGKRLDEIVVQGDV
QVEEMRKLQLEKGMVYKGLFERSS

CCB2

MSIQICNFPFHPKFAQPRQRSTRIARTENDSPQSKTSDQQLNLSVLRFTFGIPGFDE
SYLPRWIGYGFSGSLLLNHFSAPISESQMRSEALGLSLAFAFIALPYIGKFLKGSVVE
QRSLEEGEQVFISSNIGDGLKEDLAWATYVLLRNTSTIAVLISVQEGELCVRGYWNCPD
QMSKAQLHDWFKKKVDEIGLADVKETLYFPQYAGSALSILDPDGTSLFVQPLVQNTNE
PQKVNGLFLLVASTAGYAYSDKDRAGIAMAERFRG

CCB3

MTVTTSFVSFSPALMIFQKKSRRSSPNFRNRSTSLPIVSATLSHIEEAATTNLRQTN
SISELRNLSLADLDPGTAKLAIGILGPALSAFGFLFILRVMSWYPKLPVDKFPYVLAY
APTEPILVQTRKVIPLAGVDVTPVWVGLVSLSEILVGPQGLLVLSVQQQVN

CCB4

MEARIILLRIQIPWSANRQFSHPPLDFPRFIRASSSTSQPKTYEGPKPRKNLVADFIS
KNDDLVRSLPIYVGGASLLAVLFNRTVSGIAPVADASSQSRADLLALGLAVTNLLTGLV
WLSIRPKSITPVNPKGVECKVSEDLPSMVSELLWAWESLKVATCCSLVIVYNGICLI
QIGMVAESPEDKKTIVIKTKLMQGSVYRGVMKSKAQSYLANLSLYPGRSELFPPLANTQ
AVILQPLGDKGIAVIGGNTIRGFTSSDQAWISSIGEKLDATLGRYFVDSDEISRVTV

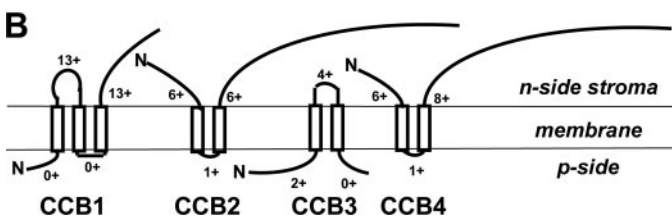


FIGURE 2. Sequence and topology of the CCB proteins of *Arabidopsis* in the thylakoid membrane. A, CCB protein sequences. Chloroplast transit peptides as predicted by ChloroP (38) are shown in gray, and transmembrane domains predicted by TMAP (39) are underlined. The last 57 amino acid residues missing in the short cDNA of CCB4 are shown in italics. B, topology of the CCB proteins based on the “positive inside rule” predictions.

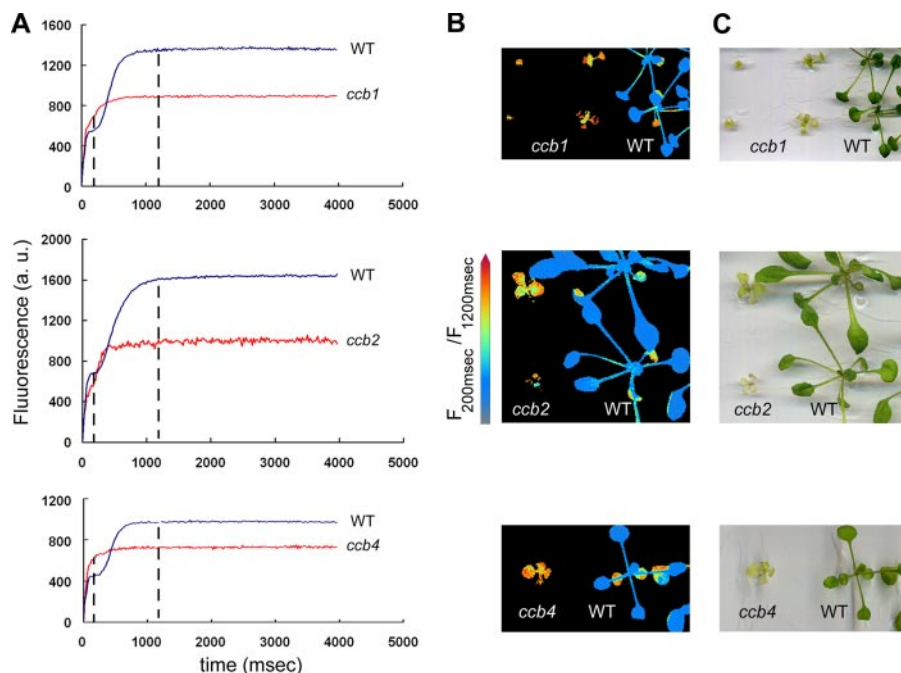


FIGURE 3. Phenotype and spectroscopic analyses of the *ccb* mutants and WT. Fluorescence induction kinetics (A), chlorophyll fluorescence imaging (B), and phenotype (C) of the 20 days old *ccb1*, *ccb2*, and *ccb4* mutant plants grown heterotrophically under continuous light of $40\text{--}50\ \mu\text{E m}^{-2}\text{ s}^{-1}$ intensity were compared with those of WT plants grown for the same time under the same conditions. Fluorescence measurements were performed after a dark period of several minutes. Pictures in B are computed from the ratio of fluorescence pictures recorded at two times (200 and 1200 ms) shown by dashed lines in A during the fluorescence rise.

(see below in this study), and the presence of CCB proteins in *Arabidopsis* chloroplast proteome studies as that of CCB3 in thylakoids (39) and of CCB4 in total chloroplast preparations (40). The topological arrangement of the CCB proteins in the thylakoid membrane (shown in Fig. 2B) was predicted based on *in silico* analysis using TMAP (41). CCB1 has three transmembrane domains, whereas CCB2, CCB3, and CCB4 have only two. The distribution of positive charges at the border of the putative transmembrane domains according to the “positive inside rule” (42) suggests the respective location of the N and C termini of each protein (Fig. 2B). The transmembrane topology predicted for the *Arabidopsis* CCB proteins was found to be similar to that predicted for the *Chlamydomonas* proteins.

Disruption of the CCB Genes in *Arabidopsis* Leads to the Impairment of Photosynthesis—To analyze the functions of the CCB proteins in *Arabidopsis*, we applied a reverse genetics approach and characterized *Arabidopsis* T-DNA lines available in public collections (see “Experimental Procedures”) carrying insertions in the *CCB1*, *CCB2*, and *CCB4* genes (Fig. 1 and supplemental Table S1). No mutants altered in the *CCB3* gene were available. The T-DNA insertion sites and genotypes were verified by PCR amplification followed by sequencing of the flanking regions (Fig. 1 and “Experimental Procedures”). The plants, homozygous for the T-DNA insertion, were nonphototrophic and seedling-lethal on a medium lacking a reduced carbon source; therefore, they were grown on sucrose-supplemented medium. Under these conditions mutant plants looked pale green and smaller compared with the wild type (Fig. 3C). Using a fluorescence imaging system, the *ccb* mutants were characterized by their

lower fluorescence yields and shorter half-times of fluorescence rise (as seen by the fluorescence rise kinetics (Fig. 3A) and the fluorescence ratios $F_{200\text{ ms}}/F_{1200\text{ ms}}$ shown in the fluorescence imaging panels (Fig. 3B)).

The CCB Proteins Are Targeted to the Chloroplasts—To verify the intracellular localization of the CCB proteins, we constructed chimeras where either transit peptides or full-length CCB proteins were fused to the N terminus of a fluorescent reporter protein. Full-length protein sequences of CCB1 and CCB3 were fused to the GFP. In the case of CCB2 and CCB4, only the transit peptide sequences were used and respectively fused either to the RFP or to GFP. The constructs were then transiently expressed in cell suspension of *Arabidopsis* protoplasts, and the fluorescence was recorded. As shown on Fig. 4, GFP and RFP fluorescence perfectly overlapped

CCB Pathway in *Arabidopsis*

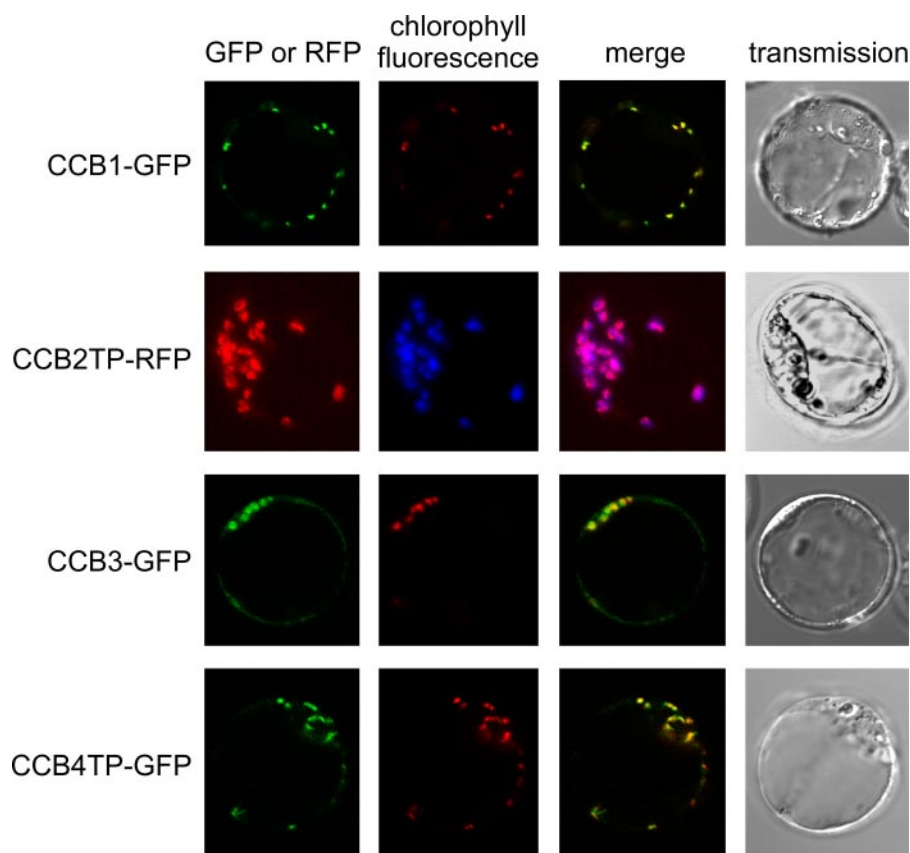


FIGURE 4. Subcellular localization of the CCB proteins. *Arabidopsis* cell suspension protoplasts were transformed with plasmids expressing the indicated translational gene fusions under the control of the constitutive ³⁵S cauliflower mosaic virus promoter. *CCB1-GFP* is the fusion of the full-length CCB1 protein to GFP, *CCB2TP-RFP* is the fusion of the CCB2 transit peptide to RFP, *CCB3-GFP* is the fusion of the full-length CCB3 to GFP, and *CCB4TP-RFP* is the fusion of the CCB4 transit peptide to GFP. Fluorescence was observed after 16 h of expression. From left to right, the first column shows the green or red fluorescence signals from the fluorescent reporter protein, the second column represents the chlorophyll red autofluorescent signal of chloroplasts, the third column is the fluorescent protein signals merged with the chlorophyll autofluorescence, and the fourth column shows the transmission images of the protoplasts.

with the auto-fluorescence of the chlorophyll, demonstrating that the CCB proteins were indeed targeted to the chloroplasts.

Heme *c*_i' Binding to Cytochrome *b*₆ Is Impaired in the *ccb* Mutants of *Arabidopsis*—We studied how the photosynthetic deficiency of the mutant plants was reflected on the protein level. The levels of accumulated cytochromes *b*₆ and *f*, determined by immunodetection using specific antibodies, were dramatically reduced to 5–10% of those in the wild type (Fig. 5, *A* and *B*, upper panels). In contrast, the representative subunits of the ATP synthase (AtpC), photosystem I (PsaC), and photosystem II (PsbA) accumulated with no obvious differences between the mutants and the wild type (Fig. 5*B*) and can be considered as controls to indicate equal loadings across the different lanes. We have previously shown that the typical biochemical signature of *c*-type cytochrome lacking its covalently bound heme cofactor is faster migration of the protein on a denaturing SDS-PAGE gel and the inability to detect the protein by the peroxidase activity of the heme (24). As shown on Fig. 5*A*, immunodetection of cytochrome *b*₆ in the *ccb* mutants shows a band that runs slightly ahead of the band in the WT or in an unrelated *b*₆*f* mutant used as a control. Moreover, the heme peroxidase activity associated with the cytochrome *b*₆

was lost for all of the *ccb* mutants (Fig. 5*A*). To exclude the possibility that the lack of peroxidase staining was due to the lower protein accumulation in the *ccb* mutant, we used additional controls consisting either of underloaded WT proteins (Fig. 5*A*, lane 4) or of an unrelated *b*₆*f* mutant (Fig. 5*A*, lane 8). Our results clearly show that reduced amounts of protein should still be sufficient to allow detection of the peroxidase activity of cytochrome *b*₆ in the *ccb* mutants if it had retained its *c*_i' heme. Fig. 5*C* shows that the peroxidase activity associated with cytochrome *f* was not altered in the *ccb* mutants, indicating that the mutations affected neither the general heme biosynthetic pathway nor the covalent heme binding to cytochrome *f*. Thus, the CCB mutations specifically prevented binding of heme *c*_i' to cytochrome *b*₆.

Functions of the CCB Proteins Are Conserved in Green Algae and Higher Plants—To confirm that the T-DNA insertions in the CCB genes were indeed responsible for the observed phenotypes, the mutants were functionally complemented by the corresponding wild type cDNAs constitutively expressed under the control of the cauliflower mosaic virus ³⁵S RNA promoter (see

“Experimental Procedures” and Fig. 6). The resulting transformants were able to grow photoautotrophically on soil and displayed a restored accumulation of cytochrome *b*₆ and heme *c*_i' binding (Fig. 5*A*). A second *CCB4* cDNA (RAFL25-07-B10) resulting from alternative splicing was also able to complement the *ccb4* mutant (Fig. 6). Surprisingly, this cDNA encodes a shorter protein devoid of the last 57 amino acid residues as compared with the best conserved *Chlamydomonas* CCB4 ortholog.

YGGT-A and YGGT-B Are Not Essential for the CCB Pathway—Among the four CCB genes, only CCB3 encodes a protein with a known conserved domain, namely, the YGGT domain. *Arabidopsis* contains three other members of the YGGT family in addition to CCB3: YGGT-A (AT5G21920), YGGT-B (AT4G27990), and YGGT-C (AT3G07430) (supplemental Table S1 and Fig. 7, *A* and *B*). They all possess chloroplast targeting sequences as predicted by ChloroP (38) (lettered in gray in Fig. 7*A*), and chloroplast proteome studies identified both YGGT-B and YGGT-C in the chloroplast envelope fraction (43, 44). The functional ortholog of *Chlamydomonas* CCB3 in *Arabidopsis* (AT5G36120) was identified on the basis of phylogenetic trees of the YGGT family because only a single YGGT member for each photosynthetic organism segregated

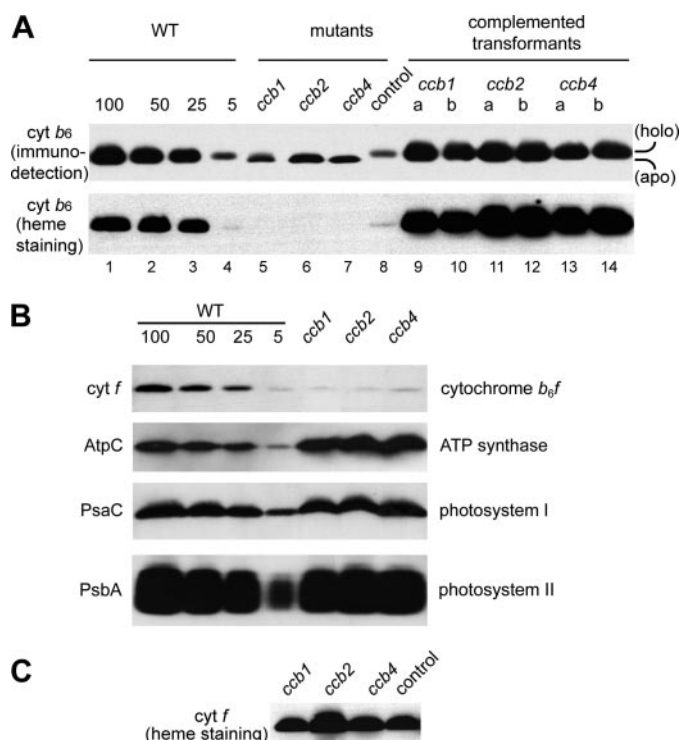


FIGURE 5. Biochemical analyses of the *ccb* mutants of *Arabidopsis* and complemented transformants. *A*, immunodetection (upper part) and heme staining (lower part) of cytochrome (cyt) *b₆* in the *ccb* mutants, complemented transformants and WT plants. On such denaturing gels, *c*-type hemes remain covalently bound to the proteins, whereas *b*-type hemes that are noncovalently bound to the proteins are lost. The cytochrome *b₆* migration position is lower for apo-cytochrome *b₆* without heme *c_i'* (apo) and slightly higher for holo-cytochrome *b₆* binding heme *c_i'* (holo) because of the additional heme mass of 616 Da. The complemented plants correspond to *ccb* mutants constitutively expressing the corresponding WT cDNA. The *ccb4* complemented plants were obtained from construct derived from RAFL21-69-K09, the cDNA clone encoding the full-length protein. Two independent transformants (a and b) were taken for each complementation analysis. An unrelated cytochrome *b₆f* mutant accumulating small amounts of cytochrome *b₆* comparable with those found in the *ccb* mutants was used as a control (control) to show that the faster mobility of cytochrome *b₆* and the lack of heme *c* bound to cytochrome *b₆* were specific for the *ccb* mutants. 100, 50, 25, and 5% of WT were loaded to enable an estimation of subunit abundance in the mutants. *B*, immunodetection of cytochrome *f*, ATP synthase subunit AtpC, photosystem I subunit PsaC, and photosystem II subunit PsbA in *ccb* mutants and WT plants. *C*, heme staining of cytochrome *f* in the *ccb* mutants. The control is the same as in *A*.

in the same cluster as the *Chlamydomonas* CCB3 (24). We decided to explore the possibility that some of the YGGT paralogs of CCB3 could participate in the CCB system because, as mentioned above, the CCB2 and CCB4 are paralog proteins probably resulting from ancestral gene duplication and both functionally involved in the CCB system. To determine whether disruption of other YGGT family members also prevented covalent binding of heme *c_i'* to cytochrome *b₆* and lead to photosynthetic deficiencies, we analyzed the phenotypes of T-DNA insertion lines for the *YGGT-A* and *YGGT-B* genes available in the public collections (supplemental Table S1 and Fig. 7B). Grown under conditions similar to those used for growing *ccb* mutants, we were unable to identify any difference either in size or in color between the wild type and the homozygous T-DNA insertion mutants for both *YGGT-A* and *YGGT-B* (Fig. 7C). The *yggt-a* and *yggt-b* mutants were able to grow under photosynthetic conditions (not shown), and as

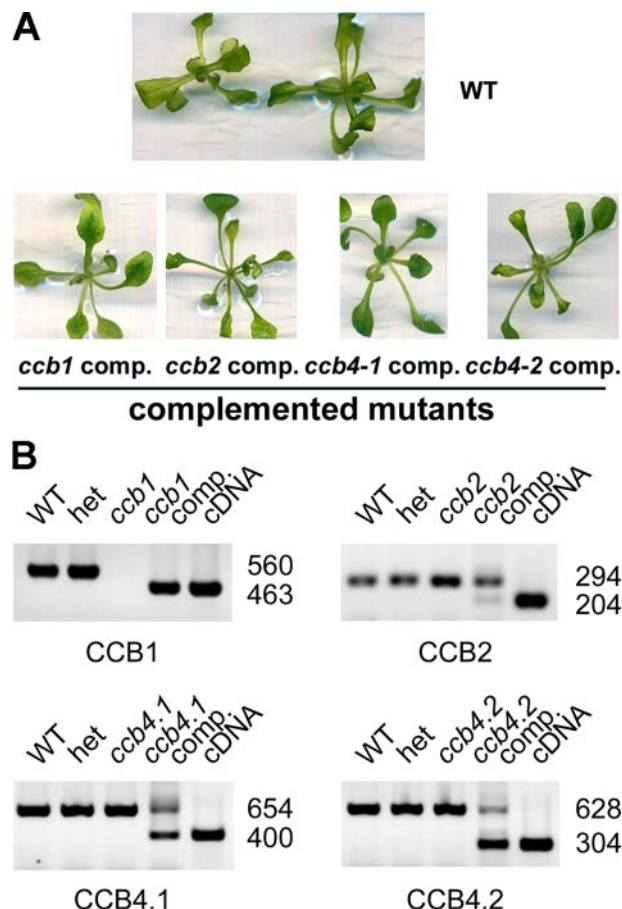


FIGURE 6. Functional complementation of the *ccb* mutants. *A*, phenotype of the homozygous *ccb1*, *ccb2*, and *ccb4* mutants constitutively expressing the corresponding wild type cDNAs as compared with WT. For the *ccb4* mutant, two different constructs encoding either a full-length (CCB4-1, derived from clone RAFL21-69-K09) or a shorter (CCB4-2, derived from clone RAFL25-07-B10) CCB4 protein were used for the complementation (comp) studies. *B*, PCR analyses confirming the presence of the exogenous cDNA in the complemented homozygous lines. Exon-specific primers (see Fig. 1 and "Experimental Procedures") were used to amplify products of different sizes using genomic DNA or cDNA as templates. Heterozygous mutant lines are named *het*.

shown in Fig. 7D, they showed no alteration in heme *c* binding to cytochromes *b₆* and *f*. That is a strong indication that neither the YGGT-A nor the YGGT-B proteins have an essential role in the CCB pathway.

DISCUSSION

Cofactor maturation pathways such as the CCB and CCS systems for *c*-heme attachment are conserved in all organisms performing oxygenic photosynthesis. The ease with which it is possible to generate and screen photosynthesis mutants in *Chlamydomonas* has been crucial in the discovery of the two *c*-type cytochrome maturation systems currently known in the chloroplasts. Genes encoding components of both system II (also known as the CCS system) and system IV (the CCB system) were first molecularly identified in *Chlamydomonas* (24, 45, 46). Studies of photosynthesis mutants in *Arabidopsis* led to the characterization of two additional system II factors involved in a redox relay necessary for the reduction of the two cysteines in the heme-binding site of apo-cytochrome *c* (47, 48). After the discovery and the initial characterization of the CCB pathway

CCB Pathway in *Arabidopsis*

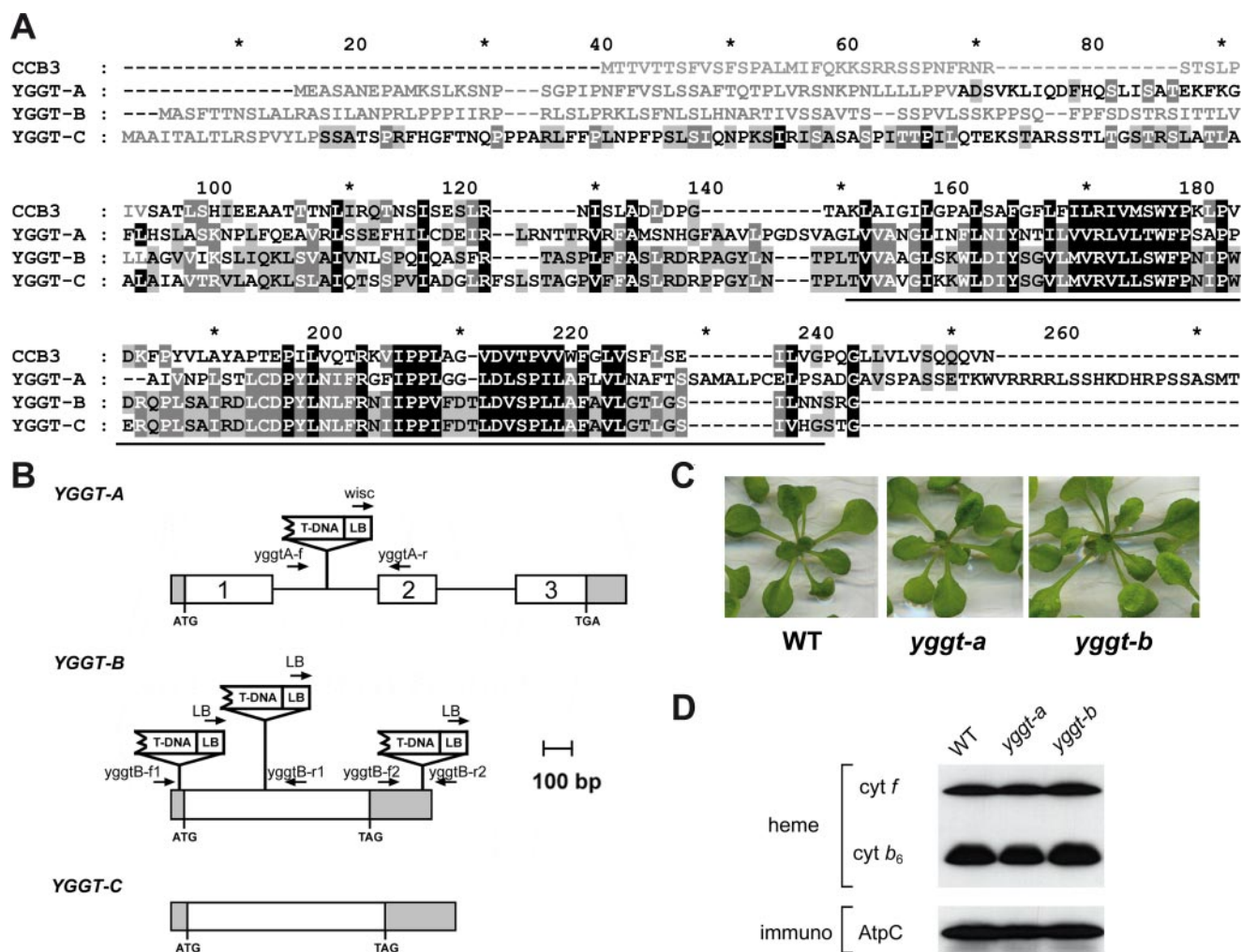


FIGURE 7. YGGT proteins. *A*, sequence alignment of the YGGT proteins of *Arabidopsis*. The YGGT domain is underlined with a black bar. Amino acids predicted to belong to the chloroplast transit peptides are lettered in gray. Shading is according to the percentage of similarity: 100% similarity is shown on a black background, 80% similarity is shown on a dark gray background, and 60% similarity is shown on a light gray background. The multiple sequence alignment was performed using ClustalW2. *B*, schematic representation of the YGGT genomic loci showing the T-DNA insertion sites. The primers used for the analyses of the T-DNA lines are indicated. *C*, phenotype of the homozygous *yggA* and *yggB* (the line carrying insertion in the coding region) mutants as compared with WT. *D*, detection of the heme peroxidase activity (heme) of cytochrome *f* and cytochrome *b₆*. The immunodetection (immuno) of AtpC in the *yggA* and *yggB* mutants as well as in the WT was used as a loading control.

in *Chlamydomonas* (24), we extended the study using available *Arabidopsis* insertion mutants and the opportunity of using fluorescent fusion proteins to identify their *in situ* subcellular localization and to contribute to further characterization of the CCB pathway.

Phylogenetic and Functional Conservation of CCBs—The four CCB proteins are conserved among all oxygenic photosynthetic organisms based on the currently existing sequence information. CCB2 and CCB4 are paralogs derived from a unique cyanobacterial ancestor (24). CCB3 is a protein of the YGGT family (European Molecular Biology Laboratory InterPro accession number IPR003425). Except for the CCB3 involved in *Chlamydomonas* in *c*-type cytochrome maturation of heme *c_i'* and one YGGT member in *Streptococcus* suggested to be involved in some division process (49), the other proteins of this family have no assigned function. *Arabidopsis* has three YGGT proteins distantly related to the CCB3 branch. All of these three proteins are predicted to be targeted to the chloroplast, and two of them, YGGT-B and YGGT-C, were identified

in biochemical studies to be present in the chloroplast envelope (43, 44), raising the question of their eventual participation in the CCB pathway. Publicly available *Arabidopsis* insertion mutant collections gave us the opportunity to test the function of YGGT-A and YGGT-B. The lack of insertion mutants for YGGT-C did not allow us to test its role. Our study indicates that neither YGGT-A nor YGGT-B are essential for the CCB maturation pathway. However, because YGGT-B and YGGT-C are very close in the phylogenetic tree (24) and could therefore have redundant functions, a double mutant (*yggB*, *yggC*) would be needed to conclude on their respective roles. This double mutant could not be generated because of the lack of insertion mutants for YGGT-C.

It was important to test whether the function of the CCB orthologs was conserved in higher plants. Indeed, the sequence similarity or the phylogenetic conservation of an open reading frame does not necessarily reflect the functional conservation of the protein. There are multiple examples of functions that were either modified or reallocated from one organism to

another (50–53). In addition, *Arabidopsis* and *Chlamydomonas* organelles have distinct pathways for mitochondrial cytochrome *c* maturation, which is performed by system I in higher plants and by system III in *Chlamydomonas* (reviewed in Ref. 54). The four CCBs are well conserved between green algae and plants, and we show that, analogous to *Chlamydomonas*, CCB1, CCB2, and CCB4 have a function in the *c*-type cytochrome maturation of heme c_i' in *Arabidopsis*. The *ccb1*, *ccb2*, and *ccb4* insertion mutants show a low accumulation of cytochrome b_6f subunits and a cytochrome b_6 in SDS-PAGE devoid of peroxidase activity with an apparent molecular mass lower than in the wild type, which corresponds to the apo-cytochrome b_6 . The apo-cytochrome *c* (f or c_e) shows also a low accumulation accounted by a short life span in the case of *ccs* mutants in *Chlamydomonas* (55). The phenotype of the *Arabidopsis* *ccb2* insertion mutant (this work) is similar to that of the recently reported *hcf208 Arabidopsis* mutant obtained by ethyl methanesulfonate mutagenesis. The mutation was identified as a glycine to arginine substitution in position 68 of the CCB2 gene that resulted in the introduction of a positive charge at the start of the first predicted transmembrane domain; it led to the loss of peroxidase activity on cytochrome b_6 in SDS-PAGE and interestingly still allowed detection of a small amount of assembled b_6f complex in blue native PAGE (56). This suggests that cytochrome b_6 lacking heme c_i' can associate with other b_6f subunits in a protease-sensitive form. Mutants with a limited protease sensitivity of b_6f complex lacking heme c_i' would be of great interest to understand the role of heme c_i' .

The functional complementation of the *ccb* mutants with the corresponding wild type cDNAs constitutively expressed under the control of the ^{35}S RNA promoter of cauliflower mosaic virus yielded transformants able to grow photoautotrophically on soil. Interestingly, a CCB4 cDNA encoding a shorter protein missing the last 57 amino acid residues was also able to successfully restore photosynthetic growth. This is particularly surprising because the missing portion of the protein encompasses several well conserved residues including a tryptophane residue. In cytochrome *c* maturation systems I and II, conserved tryptophane residues have been identified as critical in heme interactions (20, 22). In the case of CCB4, it could mean that the conserved C-terminal part of the protein does not have an essential role in the cytochrome *c'* maturation process. We also found that the expression of the CCB1 cDNA of *Chlamydomonas* in homozygous *ccb1* mutant plants led to stable transformants that were able to grow photoautotrophically on soil, providing further evidence of the conserved role of the CCB1 orthologs (data not shown).

CCB Chloroplast Localization Using Fluorescent Proteins Is Consistent with Immunodetection and Proteomics Results—In *Chlamydomonas* we showed by immunodetection in membrane fractions that the four CCB proteins were associated with the chloroplast and absent from mitochondria (24). *Arabidopsis* CCB2 and CCB3 proteins were predicted to be targeted to the chloroplast by ChloroP (38), TargetP (57), and Predotar algorithms (58), CCB1 to the chloroplast by ChloroP and TargetP but possibly to the mitochondria by Predotar, and CCB4 to the mitochondria by Predotar and TargetP. The plastid proteome data base of *Arabidopsis* indicates the presence of

CCB3 in thylakoids (39) and that of the CCB4 in total chloroplast preparations (40). Using fluorescent tagging of the four CCB proteins, we demonstrated that these proteins are targeted to the chloroplasts in *Arabidopsis* (Fig. 4).

In conclusion, we show using protein fluorescent reporters that the four CCB proteins are targeted to *Arabidopsis* chloroplasts, and we establish using *Arabidopsis* insertion mutants the generality of this cytochrome maturation pathway in higher plant chloroplasts. In addition, we test the role of two YGGT proteins for which no mutants were previously characterized. The CCB proteins define an additional maturation system for *c*-type cytochromes and are among the few that distinguish photosynthetic cells evolving oxygen from other types of living cells. The available genomic information of *Chlamydomonas* and higher plants as well as mutational studies will certainly continue to provide insight into the maturation systems of the *c*-type cytochromes and will contribute to further elucidate the role of heme c_i' in the mechanisms of electron transfer in the b_6f complex as well as the molecular nature of the signals generated by the b_6f complex and its subsequent transduction to the cytosol/nucleus.

Acknowledgments—We thank H. Barbier-Brygoo for welcoming and advising Dr. L. Lezhneva for experiments at the Institut des Sciences du Végétal, F.-A. Wollman for critical reading of the manuscript, the Nottingham *Arabidopsis* Stock Center for seeds, and the Riken Bio-Resource Center (Japan) for cDNAs. We are grateful to Jörg Meurer (Ludwig-Maximilians-Universität, Department Biologie I, Botanik, München, Germany) for providing antisera raised against cytochrome b_6 , AtpC, and PsaC. We thank M. N. Soler and S. Bolte for offering confocal microscopy facilities of the Cell Biology Platform of IFR 87 La Plante et son Environnement (CNRS, Gif sur Yvette, France).

REFERENCES

1. Merchant, S., and Sawaya, M. R. (2005) *Plant Cell* **17**, 648–663
2. de Vitry, C., and Kuras, R. (2007) in *The Chlamydomonas Sourcebook* (Stern, D., ed) 2nd Ed., Vol. II, pp. 603–637, Elsevier Science Publishers B.V., Amsterdam
3. Wollman, F.-A. (2001) *EMBO J.* **20**, 3623–3630
4. Depège, N., Bellaïre, S., and Rochaix, J. D. (2003) *Science* **299**, 1572–1575
5. Allen, J. F. (2004) *Trends Plant Sci.* **3**, 130–137
6. Finazzi, G. (2004) *J. Exp. Bot.* **55**, 383–388
7. Bellaïre, S., Barneche, F., Peltier, G., and Rochaix, J.-D. (2005) *Nature* **433**, 892–895
8. Joliot, P., Joliot, A., and Johnson, G. (2006) in *Photosystem I: The Light-Driven Plastocyanin:ferredoxin Oxidoreductase* (Golbeck, J. H., ed) Vol. 24, pp. 639–656, Springer-Verlag New York Inc., New York
9. Shikanai, T. (2007) *Annu. Rev. Plant Biol.* **58**, 199–217
10. Stroebel, D., Choquet, Y., Popot, J.-L., and Picot, D. (2003) *Nature* **426**, 413–418
11. Kurisu, G., Zhang, H., Smith, J. L., and Cramer, W. A. (2003) *Science* **302**, 1009–1014
12. Lavergne, J. (1983) *Biochim. Biophys. Acta* **725**, 25–33
13. Joliot, P., and Joliot, A. (1988) *Biochim. Biophys. Acta* **933**, 319–333
14. Yamashita, E., Zhang, H., and Cramer, W. A. (2007) *J. Mol. Biol.* **370**, 39–52
15. de Vitry, C., Desbois, A., Redeker, V., Zito, F., and Wollman, F.-A. (2004) *Biochemistry* **43**, 3956–3968
16. Zhang, H., Primak, A., Cape, J., Bowman, M. K., Kramer, D. M., and Cramer, W. A. (2004) *Biochemistry* **43**, 16329–16336
17. Alric, J., Pierre, Y., Picot, D., Lavergne, J., and Rappaport, F. (2005) *Proc.*

CCB Pathway in Arabidopsis

- Natl. Acad. Sci. U. S. A.*, **102**, 15860–15865
18. Zatsman, A. I., Zhang, H., Gunderson, W. A., Cramer, W. A., and Hendrich, M. P. (2006) *J. Am. Chem. Soc.* **118**, 14246–14247
19. Baymann, F., Giusti, F., Picot, D., and Nitschke, W. (2007) *Proc. Natl. Acad. Sci. U. S. A.* **104**, 519–524
20. Kranz, R., Lill, R., Goldman, B., Bonnard, G., and Merchant, S. (1998) *Mol. Microbiol.* **29**, 383–396
21. Nakamoto, S. S., Hamel, P., and Merchant, S. (2000) *Biochimie (Paris)* **82**, 603–614
22. Thöny-Meyer, L. (2002) *Biochem. Soc. Trans.* **30**, 633–638
23. Kuras, R., de Vitry, C., Choquet, Y., Girard-Bascou, J., Culler, D., Buschlen, S., Merchant, S., and Wollman, F.-A. (1997) *J. Biol. Chem.* **272**, 32427–32435
24. Kuras, R., Saint-Marcoux, D., Wollman, F.-A., and de Vitry, C. (2007) *Proc. Natl. Acad. Sci. U. S. A.* **104**, 9906–9910
25. Meurer, J., Meierhoff, K., and Westhoff, P. (1996) *Planta* **198**, 385–396
26. Murashige, T., and Skoog, F. (1962) *Physiol. Plant* **15**, 473–497
27. Bennoun, P., and Beal, D. (1998) in *Advances in Photosynthesis* (Rochaix, J.-D., Goldschmidt-Clermont, M., Merchant, S., eds) Vol. VII, pp. 451–458, Kluwer Academic Publishers, Dordrecht, The Netherlands
28. Seki, M., Carninci, P., Nishiyama, Y., Hayashizaki, Y., and Shinozaki, K. (1998) *Plant J.* **15**, 707–720
29. Seki, M., Narusaka, M., Kamiya, A., Ishida, J., Satou, M., Sakurai, T., Nakajima, M., Enju, A., Akiyama, K., Oono, Y., Muramatsu, M., Hayashizaki, Y., Kawai, J., Carninci, P., Itoh, M., Ishii, Y., Arakawa, T., Shibata, K., Shinagawa, A., and Shinozaki, K. (2002) *Science* **296**, 141–145
30. Reiss, B., Klemm, M., Kosak, H., and Schell, J. (1996) *Proc. Natl. Acad. Sci. U. S. A.* **93**, 3094–3098
31. Koncz, C., Martini, N., Szabados, L., Hroudá, M., Bachmair, A., and Schell, J. (1994) in *Plant Molecular Biology Manual* (Gelvin, S. B., Schilperoort, R. A., eds) Vol. B2, pp. 1–22, Kluwer Academic Publishers, Dordrecht, The Netherlands
32. Clough, S. J., and Bent, A. F. (1998) *Plant J.* **16**, 735–743
33. Hadi, M. Z., Kemper, E., Wendeler, E., and Reiss, B. (2002) *Plant Cell Rep.* **21**, 130–135
34. Mollier, P., Hoffmann, B., Debast, C., and Small, I. (2002) *Curr. Genet.* **40**, 405–409
35. Thomine, S., Lelievre, F., Debarbieux, E., Schroeder, J. I., and Barbier-Brygoo, H. (2003) *Plant J.* **34**, 685–695
36. Arnon, D. I. (1949) *Plant Physiol.* **24**, 1–13
37. Tatusova, T., and Madden, T. (1999) *FEMS Microbiol. Lett.* **174**, 247–250
38. Emanuelsson, O., Nielsen, H., and von Heijne, G. (1999) *Protein Sci.* **8**, 978–984
39. Friso, G., Ytterberg, A. J., Giacomelli, L., Peltier, J. B., Rudella, A., Sun, Q., and van Wijk, K. J. (2004) *Plant Cell* **16**, 478–499
40. Kleffmann, T., Russenberger, D., von Zychlinski, A., Christopher, W., Sjolander, K., Gruissem, W., and Baginsky, S. (2004) *Curr. Biol.* **14**, 354–362
41. Persson, B., and Argos, P. (1994) *J. Mol. Biol.* **237**, 182–192
42. Gavel, Y., Steppuhn, J., Herrmann, R., and von Heijne, G. (1991) *FEBS Lett.* **282**, 41–46
43. Rolland, N., Ferro, M., Seigneurin-Berny, D., Garin, J., Douce, R., and Joyard, J. (2003) *Photosynthesis Res.* **78**, 205–230
44. Froehlich, J. E., Wilkerson, C. G., Ray, W. K., McAndrew, R. S., Osteryoung, K. W., Gage, D. A., and Phinney, B. S. (2003) *Proteomic J. Prot. Res.* **2**, 413–425
45. Xie, Z., and Merchant, S. (1996) *J. Biol. Chem.* **271**, 4632–4639
46. Inoue, K., Dreyfuss, B. W., Kindle, K. L., Stern, D. B., Merchant, S., and Sodeinde, O. A. (1997) *J. Biol. Chem.* **272**, 31747–31754
47. Lennartz, K., Plucken, H., Seidler, A., Westhoff, P., Bechtold, N., and Meierhoff, K. (2001) *Plant Cell* **13**, 2539–2551
48. Page, M. L., Hamel, P. P., Gabilly, S. T., Zegzouti, H., Perea, J. V., Alonso, J. M., Ecker, J. R., Theg, S. M., Christensen, S. K., and Merchant, S. (2004) *J. Biol. Chem.* **279**, 32474–32482
49. Fadda, D., Pischedda, C., Caldara, F., Whalen, M. B., Anderluzzi, D., Domenici, E., and Massida, O. (2003) *J. Bacteriol.* **185**, 6209–6214
50. Caprara, M. G., Lehnert, V., Lambowitz, A. M., and Westhof, E. (1996) *Cell* **87**, 1135–1145
51. Perron, K., Goldschmidt-Clermont, M., and Rochaix, J.-D. (1999) *EMBO J.* **18**, 6481–6490
52. Alergand, T., Peled-Zehavi, H., Katz, Y., and Danon, A. (2006) *Plant Cell Physiol.* **47**, 540–548
53. Hsu, J. L., Rho, S. B., Vannella, K. M., and Martinis, S. A. (2006) *J. Biol. Chem.* **281**, 23075–23082
54. Giegé, J.-M., and Bonnard, G. (2008) *Mitochondrion* **8**, 61–73
55. Xie, Z., Culler, D., Dreyfuss, B. W., Kuras, R., Wollman, F.-A., and Merchant, S. (1997) *Genetics* **148**, 681–692
56. Lyska, D., Paradies, S., Meierhoff, K., and Westhoff, P. (2007) *Plant Cell Physiol.* **48**, 1737–1746
57. Emanuelsson, O., Nielsen, H., Brunak, S., and von Heijne, G. (2000) *J. Mol. Biol.* **300**, 1005–1016
58. Small, I., Peeters, N., Legeai, K., and Lurin, C. (2004) *Predotar: Proteomics* **4**, 1581–1590